

## Autoparametric optical drive for micromechanical oscillators

M. Zalalutdinov,<sup>a)</sup> A. Zehnder, A. Olkhovets, S. Turner, L. Sekaric, B. Ilic, D. Czaplewski, J. M. Parpia, and H. G. Craighead

Cornell Center for Materials Research, Ithaca, New York 14853-2501

(Received 21 March 2001; accepted for publication 31 May 2001)

Self-generated vibration of a disk-shaped, single-crystal silicon micromechanical oscillator was observed when the power of a continuous wave laser, focused on the periphery of the disk exceeded a threshold of a few hundred  $\mu\text{W}$ . With the laser power set to just below the self-generation threshold, the quality factor for driven oscillations increases by an order of magnitude from  $Q = 10\,000$  to  $Q_{\text{enh}} = 110\,000$ . Laser heating-induced thermal stress modulates the effective spring constant via the motion of the disk within the interference pattern of incident and reflected laser beams and provides a mechanism for parametric amplification and self-excitation. Light sources of different wavelengths facilitate both amplification and damping. © 2001 American Institute of Physics. [DOI: 10.1063/1.1388869]

Numerous applications of microelectromechanical system (MEMS) such as accelerometers,<sup>1,2</sup> force microscopes,<sup>3,4</sup> magnetometers,<sup>5</sup> mass detectors,<sup>6</sup> pressure, and temperature sensors<sup>1,7</sup> employ micromechanical oscillators as a core device. Commonly, the resonant frequency of the vibrating sensor carries the information about a parameter of interest (mass, temperature, pressure, etc.). The mechanical quality factor,  $Q$ , of the MEMS oscillator and driving-detection technique define the resolution and detection limit of a device.

Laser interferometry is a fast and highly sensitive detection method, widely used in optical MEMS.<sup>8</sup> In the present letter, we demonstrate that an interaction between a laser light beam and a MEMS structure can result in greatly enhanced performance and capabilities of the system. Self-sustained, high-frequency oscillations of disk-shaped micro-machined oscillators were actuated by focusing a continuous wave (CW) laser beam at the disk periphery. Above a threshold power,  $P_{\text{thr}} \sim 250 \mu\text{W}$ , conditions for self-generated oscillation are fulfilled (as distinct from the low-power regime where an external drive is necessary to excite vibrations). An order of magnitude increase of the quality factor (up to  $Q_{\text{enh}} = 110\,000$ ) was achieved for driven oscillations by setting the laser power just below  $P_{\text{thr}}$ .

Self-generation and  $Q$  enhancement are provided by parametric amplification. The stiffness variation,  $\Delta k$ , of the disk, required for the energy pumping is enabled by thermal expansion of the laser-heated periphery of the disk that leads to a significant tensile stress in the radial direction<sup>9</sup> (providing that the central part remains cold due to a heat sink through the short supporting pillar). Under such a stress, those vibration modes of the disk which display primarily radial bending will exhibit a higher resonant frequency in analogy with the increase of the effective spring constant of a prismatic beam under uniaxial tension.<sup>10</sup>

Light interference in a Fabry–Perot-type resonator, created by the disk and the silicon base, provides the mechanism for the position-dependent absorption of the light by the disk. Vibration of the disk leads to a periodic change of the

absorbed power, causing temperature modulation, at twice the frequency of motion. The corresponding double frequency modulation of  $k_{\text{eff}}$  provides the mechanism for parametric amplification.<sup>11</sup> Amplification is most effective when the equilibrium position of the disk coincides with the interferometric node. In this case, deflection up or down moves the disk into higher light absorption zones, causing an increase of the effective spring constant,  $k_{\text{eff}}$ .

Damping of the motion can be obtained when the equilibrium position of the disk coincides with a maximum of the interferometric pattern. For a given oscillator design, the interferometric pattern can be adjusted by tuning the laser wavelength to provide either amplification or damping of mechanical vibrations.

The parametric mechanism of self-excitation observed in our system is different from self-generation reported earlier in photovoltaic<sup>12</sup> or bimorph<sup>7,13,14</sup> MEMS oscillators. Our system does not require a built-in  $pn$  junction and is free from metallic overlayers. In turn, this facilitates operation over a wide temperature range and in various harsh environments. The enhancement of the quality factor,  $Q$ , inherent for oscillators with parametric amplification,<sup>11</sup> is a significant advantage of our system. The fact that an external driving scheme is unnecessary for self-generating vibration sensors will allow significant design simplifications, which is particularly important for MEMS sensors designed to operate remotely.

The fabrication process<sup>9</sup> for our disk-type oscillators employs a wet etch by hydrofluoric acid to undercut silicon dioxide beneath the silicon disk, which was defined in the top layer of a silicon-on insulator (SOI) wafer (250 nm thick top silicon layer and  $1 \mu\text{m}$   $\text{SiO}_2$ ), by lithography and dry etch. A scanning electron micrograph of the disk oscillators is presented in Fig. 1(a). The disk cross section is shown in Fig. 1(b), alongside the variation in light absorption due to interference. In this letter, we present the data obtained from disks with a  $40 \mu\text{m}$  outer diameter and a  $6.7 \mu\text{m}$  diameter  $\text{SiO}_2$  center pillar. Measurements were done in a vacuum chamber ( $P \sim 10^{-7}$  Torr) at room temperature using HeNe

<sup>a)</sup>Electronic mail: maxim@ccmr.cornell.edu

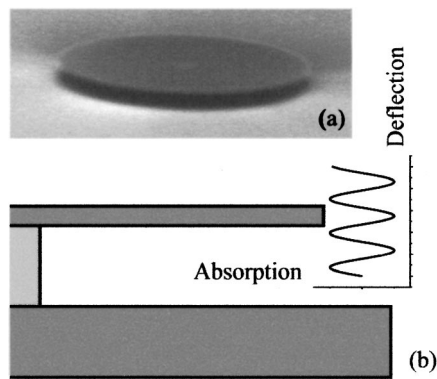


FIG. 1. (a) A scanning electron micrograph of the disk oscillator is shown. (b) A schematic vertical cross section (right half) of the disk oscillator with position-dependent absorption due to the interference effect is presented.

and  $\text{Ar}^+$  ion lasers, focused at a  $5 \mu\text{m}$  diameter spot on the periphery of the disk.

The inset in Fig. 2 demonstrates narrowing of the resonant peak and the growth of the peak amplitude (the response from the photodetector was normalized by the incident beam intensity) induced by an increase in the incident laser power. Resonant oscillations at  $890 \text{ kHz}$  ( $\gamma_{00}$  mode of vibrations<sup>15</sup>—axisymmetric mode without nodal diameters) were driven by a piezotransducer at an excitation small enough to avoid nonlinear effects. The quality factor was extracted by fitting a Lorentzian function to the measured spectrum. The results shown in Fig. 2 demonstrate an enhancement in the quality factor from 10 000 at  $100 \mu\text{W}$  of the laser power to 110 000 just below the self-generation threshold of  $250 \mu\text{W}$ . We anticipate that a combination of a surface treatment<sup>16,17</sup> and our optical parametric amplification scheme can provide even higher  $Q$  for silicon oscillators. This idea is currently under investigation.

Self-generation was observed when the CW laser power was increased above  $250 \mu\text{W}$ . The abrupt increase of the self-oscillation amplitude with a well-pronounced threshold is shown in Fig. 3.

Laser damping of the vibrations was demonstrated using

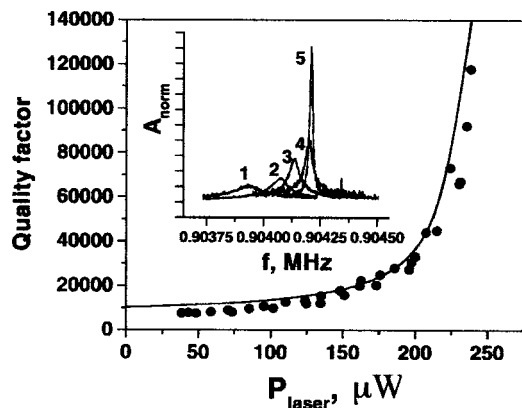


FIG. 2. Quality factor of the disk oscillator ( $40 \mu\text{m}$  outer diameter and  $6.7 \mu\text{m}$   $\text{SiO}_2$  pillar diameter) as a function of the CW laser power is shown. Light intensity was kept below the self-generation threshold, while the oscillations were driven by a piezotransducer. Solid line represents the result of theoretical calculations. Inset shows the shape of the spectra acquired for different values of laser power:  $58 \mu\text{W}$  (line 1),  $124 \mu\text{W}$  (line 2),  $162 \mu\text{W}$  (3),  $198 \mu\text{W}$  (4), and  $235 \mu\text{W}$  (5) (the curves are normalized by the light intensity and the piezovoltage).

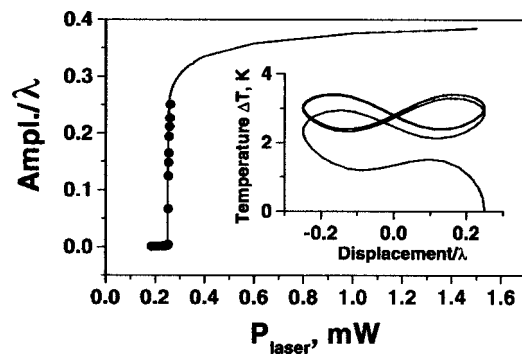


FIG. 3. Amplitude of the self-oscillating peak as a function of the CW laser power is shown. Circles represent experimental data (normalized). The result of the theoretical calculations for the amplitude of vibration due to parametric self-excitation is shown by the solid line. Inset demonstrates modulation of the local overheating (disk temperature under the laser beam) caused by the motion within the interferometric pattern. The laser intensity and the ratio of temperature diffusion time to the period of oscillation define the loop area, which is related to the energy income per cycle [ $\Delta T \sim \Delta k$ , Eq. (4)].

two laser beams with different wavelengths [ $633 \text{ nm}$  (red) HeNe and  $458 \text{ nm}$  (blue)  $\text{Ar}^+$  ion laser]. The thicknesses of both the silicon and the sacrificial oxide layers were chosen so that at the rest position of the disk, the arrangement of the interferometric fringes for red and blue light was complementary, i.e., “red” nodes coincide with “blue” antinodes. Initially, by applying the CW red laser beam ( $P_{\text{HeNe}} = 400 \mu\text{W}$ ), the disk was set into a self-generation regime. When the  $\text{Ar}^+$  laser beam was superimposed at the same spot as the red laser, a decay of the self-oscillations, down to cessation of motion was observed, as shown in Fig. 4.

The oscillations of the disk can be modeled by combining detailed finite element (FEM) simulations with a simple one degree of freedom model in which the disk is treated as a mass on a nonlinear spring, and the thermal problem is simplified to a lumped mass with conductive cooling. Expressing time and displacement in dimensionless units  $t = \omega_0 \tau$  and  $z = x/\lambda$ , respectively, where  $\omega_0$  is the natural frequency of the relevant mode, and  $\lambda$  is the wavelength of the red laser, the thermal and mechanical problems can be written as

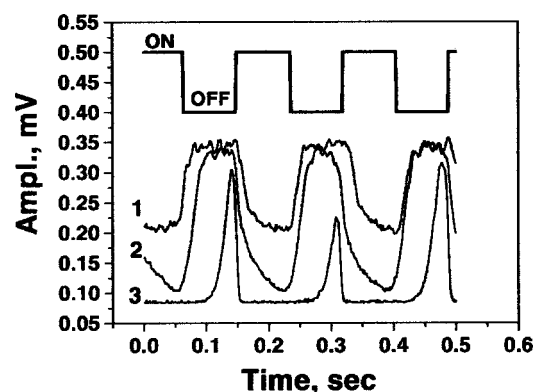


FIG. 4. Demonstration of the laser damping of mechanical vibrations. The self-generation induced by the CW He–Ne laser ( $P_{\text{HeNe}} = 400 \mu\text{W}$ ) is periodically suppressed by applying a modulated  $\text{Ar}^+$  ion laser beam to the same spot. Meander on the top of the graph shows the  $\text{Ar}^+$  laser duty cycle. The lines below show time dependence of the ac signal from a photodetector (proportional to the amplitude of self-oscillations) for different intensity of the  $\text{Ar}^+$  laser beam:  $195 \mu\text{W}$  (line 1),  $230 \mu\text{W}$  (2), and  $790 \mu\text{W}$  (3).

$$\omega_0 \dot{T}(t) = Aq(t) - BT(t), \quad (1)$$

$$\ddot{z}(t) = -\dot{z}(t)/Q - (1 + \Delta k(t)/k_0)z(t) - \beta(1 + \Delta k(t)/k_0)^3 z^3(t), \quad (2)$$

$$\Delta k(t)/k_0 = C(2\omega_0)T(t), \quad (3)$$

$$q(t) = q_0 f(z(t)), \quad (4)$$

where  $T(t)$  and  $q(t)$  are the time dependence of the heat-induced temperature difference and the absorbed laser power respectively,  $Q$  is the quality factor,  $\Delta k(t)/k_0$  is the fractional change in effective stiffness, and  $q_0$  is the incident laser power. The light intensity distribution function,  $f(z)$ , represents the position-dependent heat absorption and couples the thermal and mechanical problems. We assume in our model that

$$f(z) = 2 \sin^2(2\pi z). \quad (5)$$

Detailed FEM simulations are used to extract the parameters  $A$ ,  $B$ ,  $C$ , and  $\beta$ . The parameters  $A$  and  $B$  are estimated from the temperature distribution, assuming that 25% of the laser light intensity is absorbed by the Si disk.<sup>18</sup>

The change in stiffness due to laser heating,  $C$ , is estimated from results of the FEM simulation by computing the change in resonant frequency at different points in the transient heating cycle, corresponding to different disk displacements. Note that at high frequencies, the temperature modulation away from the point of absorption diminishes considerably, and thus  $C$  is a decreasing function of frequency. We find  $C(2\omega_0) \approx C(0)/3$  for  $\omega_0 = 0.89$  MHz.

The cubic nonlinearity parameter,  $\beta$ , is estimated by loading the disk with a uniform pressure,  $p$ , and fitting the displacement,  $z$ , at the edge of the disk to  $p = k(z + \beta z^3)$ . We find  $\beta = 2.3$ .

The computed temperature variation of the ‘‘hot spot’’ under the laser beam is shown in the inset of Fig. 3. In this simulation, the laser power was 250  $\mu$ W and system was allowed to evolve freely from an initial deflection. Self-oscillations with the amplitude  $0.25 \lambda$  become a stable state of the system after a few periods.

The calculated amplitude of self-generation is plotted against the incident CW laser power as the solid line in Fig. 3. The threshold value of 250  $\mu$ W found by simulation for the onset of the self-sustained oscillation corresponds very well to the experimental data. Above the threshold power, the amplitude of motion is self-limited by the neighboring peaks of  $f(z)$ .

For a light intensity below the self-generation threshold, the effect of the laser light on free vibration is to slow down the decay in motion. This was simulated by computing the decay in oscillation for various values of  $q_0$  [Eq. (4)] and using the logarithmic decrement method to determine  $Q$ . Results of the model agree closely with the experimental data, as shown in Fig. 2.

Note that unlike the textbook cases of parametric amplification,<sup>11</sup> the magnitude of pumping in our system de-

pends on the displacement via the function  $f(z)$ . The question remains as to whether infinitely small vibrations are amplified or if there is a threshold of the initial amplitude, below which the vibration decays. This problem and the closely related effect of the thermal noise and external vibrations are also the subject of current theoretical and experimental study.

In conclusion, an order of magnitude quality factor enhancement (up to  $Q_{\text{enh}} \sim 110\,000$ ) was realized for a micro-mechanical disk-shaped oscillator, by interaction with a spatially modulated CW laser beam. Self-generation of the disk was observed when the laser power exceeded a threshold value of 250  $\mu$ W. We attribute these effects to parametric amplification of mechanical vibration by laser light. Our structure was designed so that the interferometric pattern of a red light (He-Ne) was suitable for parametric self-excitation. Laser damping was demonstrated using a laser source of a different wavelength ( $\text{Ar}^+$ ).

The authors are grateful to Ai-Chi Chien for assistance with the FEM computations and to the staff at Cornell Nanofabrication Facility for generous aid in fabrication. This work was supported by the Cornell Center for Materials Research (CCMR), a Materials Research Science and Engineering Center of the National Science Foundation (DMR-0079992). Particular acknowledgment is made of the use of the Research Computing Facility of the CCMR.

- <sup>1</sup>J. D. Zook, W. R. Herb, C. J. Bassett, T. Stark, J. N. Schoess, and M. L. Wilson, *Sens. Actuators A* **83**, 270 (2000).
- <sup>2</sup>A. Partridge, J. K. Reynolds, B. W. Chui, E. M. Chow, A. M. Fitzgerald, L. Zhang, N. I. Maluf, and T. W. Kenny, *J. Microelectromech. Syst.* **9**, 58 (2000).
- <sup>3</sup>D. Sarid, *Scanning Force Microscopy With Applications to Electric, Magnetic and Atomic Forces*, (Oxford University Press, New York, 1994).
- <sup>4</sup>J. A. Sidles, J. L. Garbini, K. J. Bruland, D. Rugar, O. Zuger, S. Hoen, and C. S. Yannoni, *Rev. Mod. Phys.* **67**, 249 (1995).
- <sup>5</sup>M. Lohndorf, J. Moreland, P. Kabos, and N. Rizzo, *J. Appl. Phys.* **87**, 5995 (2000).
- <sup>6</sup>B. Ilic, D. Czaplowski, H. G. Craighead, P. Neuzil, C. Campagnolo, and C. Batt, *Appl. Phys. Lett.* **77**, 450 (2000).
- <sup>7</sup>N. A. D. Stokes, R. M. A. Fatah, and S. Venkatesh, *Sens. Actuators A* **21**, 369 (1990).
- <sup>8</sup>D. W. Carr, L. Sekaric, and H. G. Craighead, *J. Vac. Sci. Technol. B* **16**, 3281 (1998).
- <sup>9</sup>M. Zalalutdinov, A. Olkhovets, A. Zehnder, B. Ilic, D. Czaplowski, H. G. Craighead, and J. M. Parpia, *Appl. Phys. Lett.* **78**, 3142 (2001).
- <sup>10</sup>S. Timoshenko, D. H. Young, and W. Weaver, *Vibration Problems in Engineering*, 4th ed. (Wiley, New York, 1994), pp. 453–455.
- <sup>11</sup>W. H. Louisell, *Coupled Mode and Parametric Electronics* (Wiley, New York, 1960).
- <sup>12</sup>J. D. Zook, D. W. Burns, W. R. Herb, H. Guckel, J. W. Kang, and Y. Ann, *Sens. Actuators A* **52**, 92 (1996).
- <sup>13</sup>A. V. Churenkov, *Sens. Actuators A* **39**, 141 (1993).
- <sup>14</sup>K. Hane and K. Suzuki, *Sens. Actuators A* **51**, 179 (1996).
- <sup>15</sup>P. M. Morse *Vibration and Sound* 2nd ed. (McGraw-Hill, New York, 1948), pp. 172–216.
- <sup>16</sup>K. Y. Yasumura, T. D. Stowe, E. M. Chow, T. Pfafman, T. W. Kenny, B. C. Stipe, and D. Rugar, *J. Microelectromech. Syst.* **9**, 117 (2000).
- <sup>17</sup>J. Yang, T. Ono, and M. Esashi, *Appl. Phys. Lett.* **77**, 3860 (2000).
- <sup>18</sup>*American Institute of Physics Handbook*, 3rd ed., edited by D. E. Gray (McGraw-Hill, New York, 1972), pp. 6-118–6-156. Absorption calculation assumes optical properties of pure Si at 620 nm.